

## A Windstorm in the Lee of a Gap in a Coastal Mountain Barrier

CLIFFORD F. MASS

*Department of Atmospheric Sciences, University of Washington, Seattle, Washington*

STEVE BUSINGER

*Department of Meteorology, University of Hawaii at Manoa, Honolulu, Hawaii*

MARK D. ALBRIGHT

*Department of Atmospheric Sciences, University of Washington, Seattle, Washington*

ZENA A. TUCKER

*United States Air Force, Las Vegas, Nevada*

(Manuscript received 15 February 1994, in final form 5 July 1994)

### ABSTRACT

This paper describes a localized windstorm that struck some areas of northwest Washington State on 28 December 1990 with winds exceeding  $45 \text{ m s}^{-1}$ , resulting in extensive property damage, treefalls, and power outages. Arctic air, originating within the interior of British Columbia, descended into a mesoscale gap in the Coast/Cascade Mountains and then accelerated ageostrophically to the west. This gap acceleration is explained quantitatively by a three-way balance among the pressure gradient force, friction, and inertia. The flow maintained its integrity as a narrow current of high-speed air as it exited the gap and subsequently accelerated over water. Troughing in the lee of the Cascade Mountains enhanced the horizontal pressure gradient over northwest Washington; this pressure gradient approximately balanced frictional drag resulting in only minimal acceleration. Farther south the flow decelerated as the current spread out horizontally.

### 1. Introduction

During the morning hours of 28 December 1990, strong winds exceeding  $45 \text{ m s}^{-1}$  struck portions of northwest Washington State causing extensive treefalls, two deaths, widespread power outages,<sup>1</sup> severe damage to several marinas, the loss of hundreds of boats, considerable destruction of oyster beds, and damage to numerous buildings. These strong winds can be traced to the outflow of arctic air from a mesoscale gap in the Coast/Cascade Mountains near the border between British Columbia and Washington. After exiting the gap, the arctic air then headed southward, producing northerly flow of  $15\text{--}40 \text{ m s}^{-1}$  over the southern Strait of Georgia, the eastern Strait of Juan de Fuca, and the Puget Sound lowlands (Fig. 1).

<sup>1</sup> Nearly 150 000 residences lost power in western Washington due to the storm.

*Corresponding author address:* Prof. Clifford F. Mass, Department of Atmospheric Sciences, AK-40, University of Washington, Seattle, WA 98195.

The most significant terrain feature of the region is the barrier formed by the Cascade and Coast Ranges (Fig. 1a). With general crest levels of 2000–3000 m, these mountains form a nearly continuous barrier that impedes the westward movement of cold air from the interior. The most significant mesoscale gap in this orography, associated with the Fraser River valley, connects the interior of southern British Columbia with the lowlands of western Washington and southwestern British Columbia. Approximately 150 km to the west, lower coastal mountains roughly parallel the Cascade and Coast Ranges. The most prominent components of the coastal mountains are the Olympic Range, located to the west of Puget Sound, and the mountains of Vancouver Island. Figure 1b, which presents more detailed topography for northwest Washington, shows that northeasterly flow exiting the Fraser Gap passes over a complex array of land, water, and islands.

The cold, dry outflow from the Fraser Gap moves into northwest Washington as a well-defined current that can spread westward into the Strait of Juan de Fuca or southward over Puget Sound (Overland and Walter 1981). The San Juan Islands (near the eastern end of the Strait of Juan de Fuca), as well as Guemes Island,

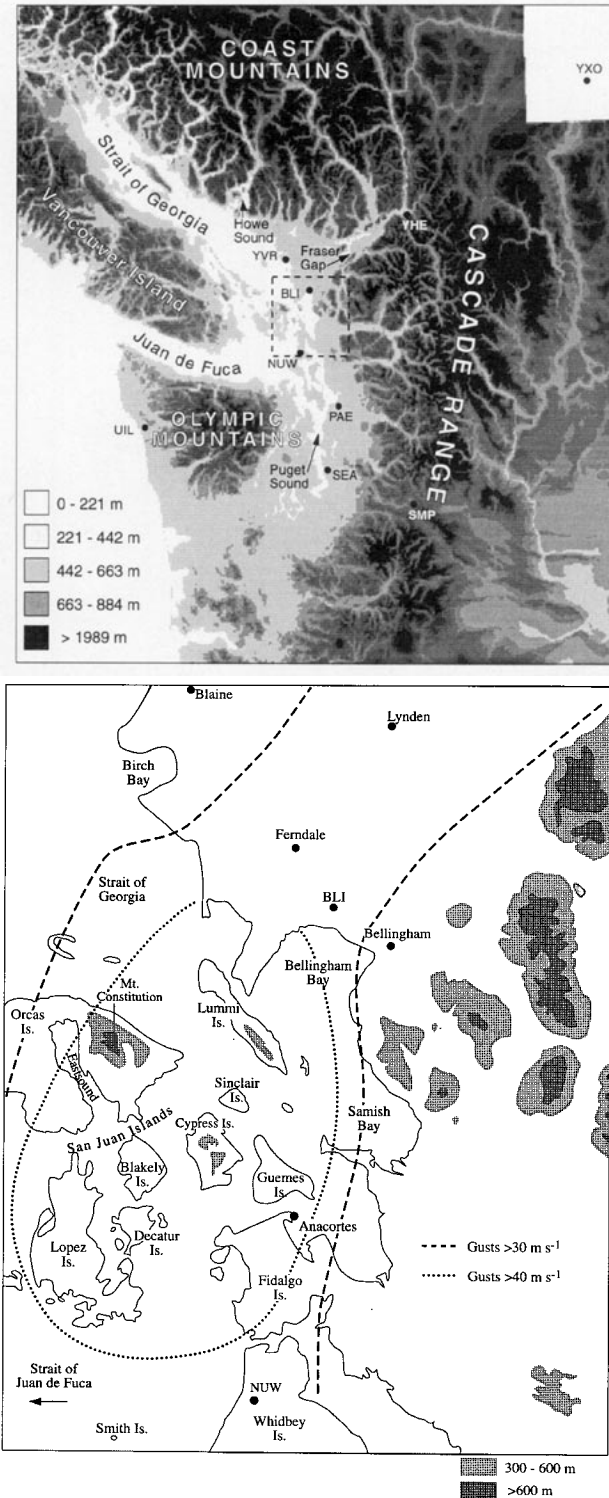


FIG. 1. Topography and geographical locations for the (a) Pacific Northwest and (b) northwest Washington. The boundaries of extreme wind (gusts exceeding  $40 \text{ m s}^{-1}$ , 1-min average winds of  $30\text{--}35 \text{ m s}^{-1}$ ) and strong wind (gusts exceeding  $30 \text{ m s}^{-1}$ , 1-min average winds of  $20\text{--}30 \text{ m s}^{-1}$ ) are shown by the dotted and dashed lines, respectively. Surface stations shown are Seattle-Tacoma Airport (SEA), Stampede Pass (SMP), Quilayute (UIL), Whidbey Island Naval Air Station (NUW), Bellingham (BLI), Vancouver (YVR), Hope (YHE), and Vernon (YXO).

Fidalgo Island, and northern Whidbey Island, are frequently affected by the strong, often damaging, northeasterly winds produced by Fraser Gap wind events. In addition to the Fraser Gap, cold air also crosses the Coast Range in narrower gaps such as Howe Sound, located to the north of Vancouver (Jackson and Steyn 1994). However, as noted in Ferber et al. (1993), Fraser Gap flow is the most important source of cold, arctic air for the lowlands of western Washington and is associated with most significant snow events over the region.

Strong ( $>25 \text{ m s}^{-1}$ ) outflows of arctic air through the Fraser Gap into western Washington occur approximately once or twice a year. Such gap wind events are associated with a specific synoptic evolution that results in a large pressure gradient between a cold arctic anticyclone over the interior of southern British Columbia and lower pressure over western Washington (Dickey and Wing 1963; Ferber et al. 1993). Aloft, Fraser Gap windstorms are associated with the amplification of a meridional 500-mb ridge into Alaska and the Yukon Territory and the southeastward passage of a short-wave trough into the Pacific Northwest. The upper-level ridging and lower-tropospheric cold advection behind such short-wave troughs result in large low-level pressure increases over the southern interior of British Columbia that push cold air through the Fraser Gap into western Washington.

Extreme northeasterly wind events, in which wind speeds exceed  $40 \text{ m s}^{-1}$ , are relatively infrequent, occurring on the average every 5–10 years. Paradoxically, such storms have been more numerous of late, with the strong event of 28 December 1990, preceded by the nearly equal northeasterly wind storms of 18 December 1990 and 1 February 1989. Although the general character of these storms is quite similar, some differences in the current of strong winds are observed. For example, the 28 December 1990 event produced far more damage on Guemes and Fidalgo Islands than the somewhat weaker event two weeks before. Based on discussions with numerous long-term residents, the 28 December 1990 windstorm was the most intense in living memory at most locations.

The remainder of this paper describes the synoptic and mesoscale evolution of the 28 December 1990 arctic air intrusion. Particular attention will be given to documenting and providing a physical explanation for the strongest winds. Specifically, this paper examines the effects of gaps, the formation of a lee trough, discontinuities in surface roughness and surface fluxes, channeling, and various microscale effects on the wind distribution during the event.

## 2. Distribution of strong winds and damage

During the windstorm of 28 December 1990, northeasterly winds gusting to  $20\text{--}30 \text{ m s}^{-1}$  ( $40\text{--}60 \text{ kt}$ ) occurred over much of the lowlands of western Washing-

TABLE 1. Observations at Bellingham, Washington, on 27–29 December 1990.

Date	Time (UTC)	Sky	VIS (mi)	WEA	SLP (mb)	<i>T</i> (°F)	DP (°F)	WDIR	WSPD (kt)	GST (kt)	PEAK WDIR	PEAK SPD
27	2353	OV	15		1003.8	40	34	210	05			
28	0250	OV	7	R-	1002.8	39	35	150	07			
28	0350	OV	5	R-F	1003.2	36	34	010	11			
28	0450	OV	5	R-S-F	1003.2	35	34	040	05			
28	0550	OV	3	S-	1004.2	28	24	040	20	32		
28	0851	BK	7		1009.1	20	03	030	35	55	030	55
28	1151	BK	7		1014.5	16	-03	040	30	46	030	52
28	1451	CL	7		1019.7	11	-10	030	28	43	030	51
28	1754	CL	40		1024.8	11	-13	040	25	41	040	45
28	2054	CL	40		1025.9	11	-15	050	24	39	050	42
28	2354	CL	40		1025.9	12	-17	050	20	33		
29	0250	CL	15		1026.9	11	-16	050	20	34		
29	0550	CL	15		1028.6	11	-15	040	16	33		
29	0852	CL	15		1029.9	12	-16	050	17	25		
29	1151	CL	15		1031.2	11	-13	040	12			

Legend: VIS (visibility), WEA (current weather), SLP (sea level pressure), *T* (temperature), DP (dewpoint), WDIR (wind direction), WSPD (wind speed), GST (wind gust), PEAK (highest wind speed during the hour).

ton. Such winds by themselves would have caused considerable damage and power outages, in part due to the relative infrequency of strong northerly winds over this region. As noted in the introduction, considerably stronger winds, some exceeding  $45 \text{ m s}^{-1}$ , were observed over portions of northwest Washington. The description of the wind and damage provided below is based upon the operational meteorological network, discussions with over two dozen National Weather Service spotters and local observers, review of local newspapers, and information from local public agencies.

As illustrated by the wind observations from Bellingham Airport (BLI) at the western terminus of the Fraser Gap (Table 1, Fig. 14), strong northeasterly winds entered northwest Washington at approximately 0600 UTC 28 December and remained strong for approximately 24 h. As shown in Fig. 1b, the strong flow was limited to a relatively narrow, well-defined current whose boundaries remained quite sharp tens of kilometers beyond the terminus of the gap. Over land, the core of strongest winds (gusts exceeding  $40 \text{ m s}^{-1}$ , 1-min average winds of  $30\text{--}35 \text{ m s}^{-1}$ ) was centered along an axis stretching through the towns of Lynden and Ferndale, with wind speed rapidly diminishing toward Blaine to the north and downtown Bellingham to the south. Numerous large trees were uprooted and power was lost throughout this swath. Approximately 3 km north-northeast of BLI at the Whatcom County Transportation Services Department a wind gust of  $50.5 \text{ m s}^{-1}$  (101 kt) was reported at approximately 0800 UTC 28 December, accompanied by the loss of the roof of a truck storage shed.<sup>2</sup> BLI, on the southern

side of the swath and sheltered by tall trees, reported sustained winds of 35 kt ( $17.5 \text{ m s}^{-1}$ ) and a maximum gust of 55 kt ( $27.5 \text{ m s}^{-1}$ ); however, the wind was strong enough at one part of the airport to blow in the north wall of a helicopter hanger. Although wind speeds were attenuated inland of downtown Bellingham, there was considerable damage along the shore. Two barges were torn from their moorings and sent adrift, later grounding a few miles south of the city. A Georgia Pacific boiler stack (24.4 m tall, 6.4 mm steel, 1.5 m across) was snapped off 30 ft from the top.

The northeasterly current maintained its integrity and strengthened as it passed over the water. Two observers on the northern, relatively flat portion of Lummi Island reported northeasterly winds exceeding  $44 \text{ m s}^{-1}$  (87 kt, 100 mph) during the storm.<sup>3</sup> These winds resulted in massive treefalls, damage to homes, and extensive power outages on the island. Further to the south, Gumes Island was particularly hard hit, with massive treefalls over much of the island. According to local residents, damaging northerly winds began to strike Gumes Island just after 0000 LST (0800 UTC 28 December) and reached their peak around 1200 UTC 28 December. Figure 2, which presents a map of the tree damage based on a survey by one of the authors and several residents, shows that tree loss occurred predominantly on the windward side of the island. The most severe tree damage occurred in swaths approximately 200 m long, 50 m wide, and separated by 0.5 km, that were oriented approximately in the direction

above the ground. Considering the exposure, some mechanical acceleration of the incoming airstream is possible.

<sup>3</sup> One individual measured a gust of  $47 \text{ m s}^{-1}$  (93 kt, 107 mph) and the other observer's anemometer reached its maximum value of  $44 \text{ m s}^{-1}$  (87 kt, 100 mph).

<sup>2</sup> The anemometer was located on the east (windward) side of the building approximately 7.5 ft above a roof which itself was 24 ft

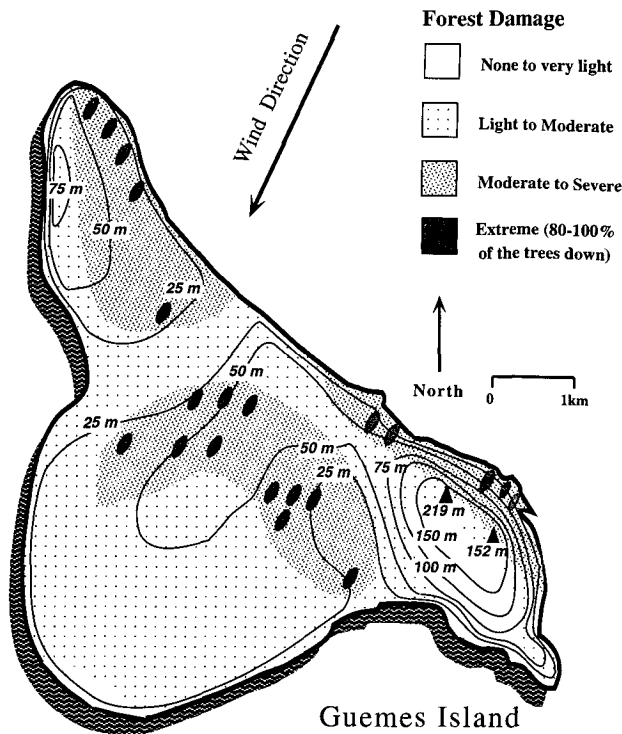


FIG. 2. Treefall survey for Guemes Island. Light to moderate damage indicates the loss of small to large tree branches, while moderate to severe damage was associated with the scattered downing of trees.

of the prevailing wind. An aerial photograph of a damage swath is shown in Fig. 3. Outside of the swaths scattered damage occurred. Such swathlike distribution of the major treefalls was found at other locations during the storm (Terry L. Patton 1992, personal communication) and is reminiscent of the narrow damage tracks observed during severe downslope windstorms in the lee of the Cascades (Mass and Albright 1985) and the Rockies (Bedard 1990). The unusual nature of the wind storm at Guemes is suggested by several facts: 1) many of the fallen trees were over one hundred years old, 2) long-time residents of the island could not remember a storm of similar magnitude, 3) the previous month was not excessively wet (which might have contributed to enhanced tree loss). Although anemometer data was not available on Guemes Island during this event, the severe nature of the damage is consistent with F2 damage on the Fujita scale, corresponding to wind speeds of  $49\text{--}68\text{ m s}^{-1}$  ( $98\text{--}136\text{ kt}$ ).

Immediately to the south of Guemes Island, very strong winds struck northern Fidalgo Island, where extensive loss of trees and numerous power outages occurred. Particularly hard hit was Anacortes, on the north shore of Fidalgo Island, where several dozen boats, approximately two-dozen boat houses, and many of the docks were destroyed or heavily damaged at the Cap Sante and Wyman Marinas (Fig. 4). In addition,

the windows of a Anacortes restaurant (Boomer's Landing) that faced north toward Guemes Island were blown in. A well-sited anemometer in Anacortes recorded sustained winds of  $35\text{ m s}^{-1}$  ( $70\text{ kt}$ ) with gusts in excess of  $44\text{ m s}^{-1}$  ( $87\text{ kt}$ )—the maximum speed possible for the unit<sup>4</sup>—from approximately 1100 to 1700 UTC 28 December. Damage and high wind reports decreased rapidly approximately 10 km east of Anacortes. On the western side of Fidalgo Island a man was killed when a tree fell on his car. Immediately south of Fidalgo, Deception Pass State Park on northern Whidbey Island experienced “the greatest devastation the park ever had” with motorists in the park trapped by downed trees.

Several of the islands west of Guemes Island also experienced extreme winds, massive treefalls, and complete loss of power. For example, as a result of falling trees more than one hundred power poles were toppled on Decatur Island. On Lopez Island several anemometers both on the northeast shore and in the interior measured winds of  $43\text{--}46\text{ m s}^{-1}$  ( $87\text{--}92\text{ kt}$ ) and the ferry dock on the north side of the island was extensively damaged. On the eastern side of Orcas Island, hundreds of large trees were lost on the windward slopes of Mount Constitution. Reports of winds and damage decreased west of Lopez Island; for example, Friday Harbor airport on the eastern side of San Juan Island reported a maximum gust of only  $18\text{ m s}^{-1}$  ( $35\text{ kt}$ ) during the height of the storm and damage reports on that island decreased rapidly to the west.

Wind speeds decreased considerably south of Lopez and Fidalgo Islands. For example, Whidbey Island Naval Air Station (NUW) reported a maximum gust of  $25\text{ m s}^{-1}$  ( $51\text{ kt}$ ), whereas at Smith Island, approximately 15 km to the west, the peak wind reached only  $22\text{ m s}^{-1}$  ( $44\text{ kt}$ ). Further south over the Puget Sound lowlands, northerly winds gusting to  $20\text{--}25\text{ m s}^{-1}$  were common and were associated with treefalls, power outages, and damage to north-facing marinas and docks.

### 3. Description of the evolution of the 28 December 1990 windstorm

#### a. Synoptic and mesoscale analyses

At 1200 UTC 27 December 1990, approximately 18 h before the windstorm began, the Pacific Northwest was under northwesterly flow at 500 mb, with a short-wave trough to the north over British Columbia (Fig. 5a). At both 850 mb and the surface (Figs. 5b,c), a trough associated with an arctic front extended westward across southern Alberta and British Columbia and

<sup>4</sup> The anemometer was located about 40 ft above ground level and was mounted on a mast affixed to the northern side of the roof.

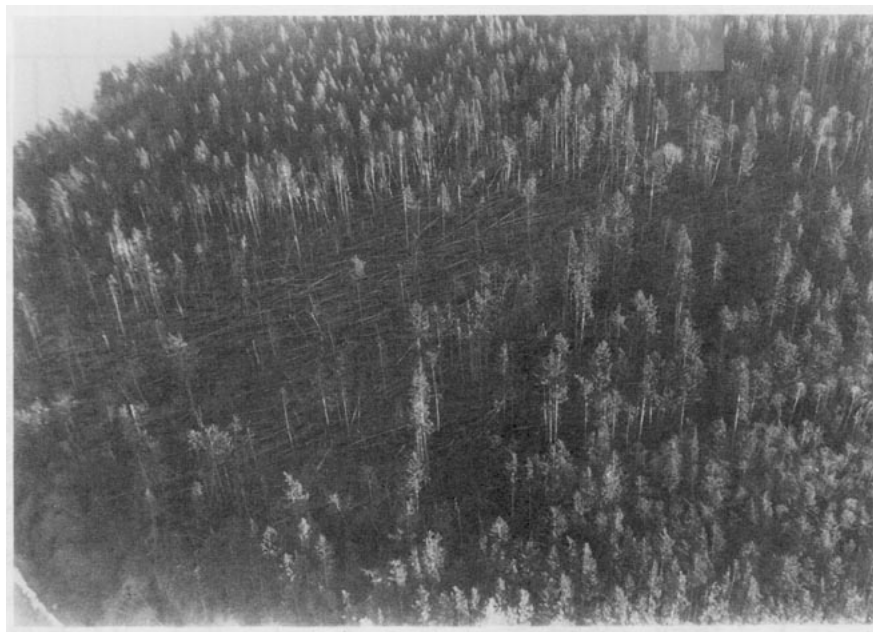


FIG. 3. Aerial photograph of a damage swath on Guemes Island.  
Photo courtesy of Win Anderson.

then northwestward along the British Columbian and southeast Alaskan coasts. At the surface there was a zone of large pressure gradient and rapidly falling temperature between the arctic front and an anticyclone centered over the Yukon Territory. This baroclinic zone extended up through 850 mb, where temperatures ranged from approximately  $-5^{\circ}\text{C}$  over northern Wash-

ington and southern British Columbia to less than  $-30^{\circ}\text{C}$  over northern British Columbia and the Northwest Territories.

By 0000 UTC 28 December the 500-mb short-wave trough had sharpened and moved south to Washington (Fig. 6a). At 850 mb (Fig. 6b) the trough had drifted southward and deepened into a closed low centered



FIG. 4. Two boats washed onto the rocks near Wyman Marina in Anacortes. The view faces north and looks across Guemes channel. Photo courtesy of Scott Terrell, Skagit Valley Herald.

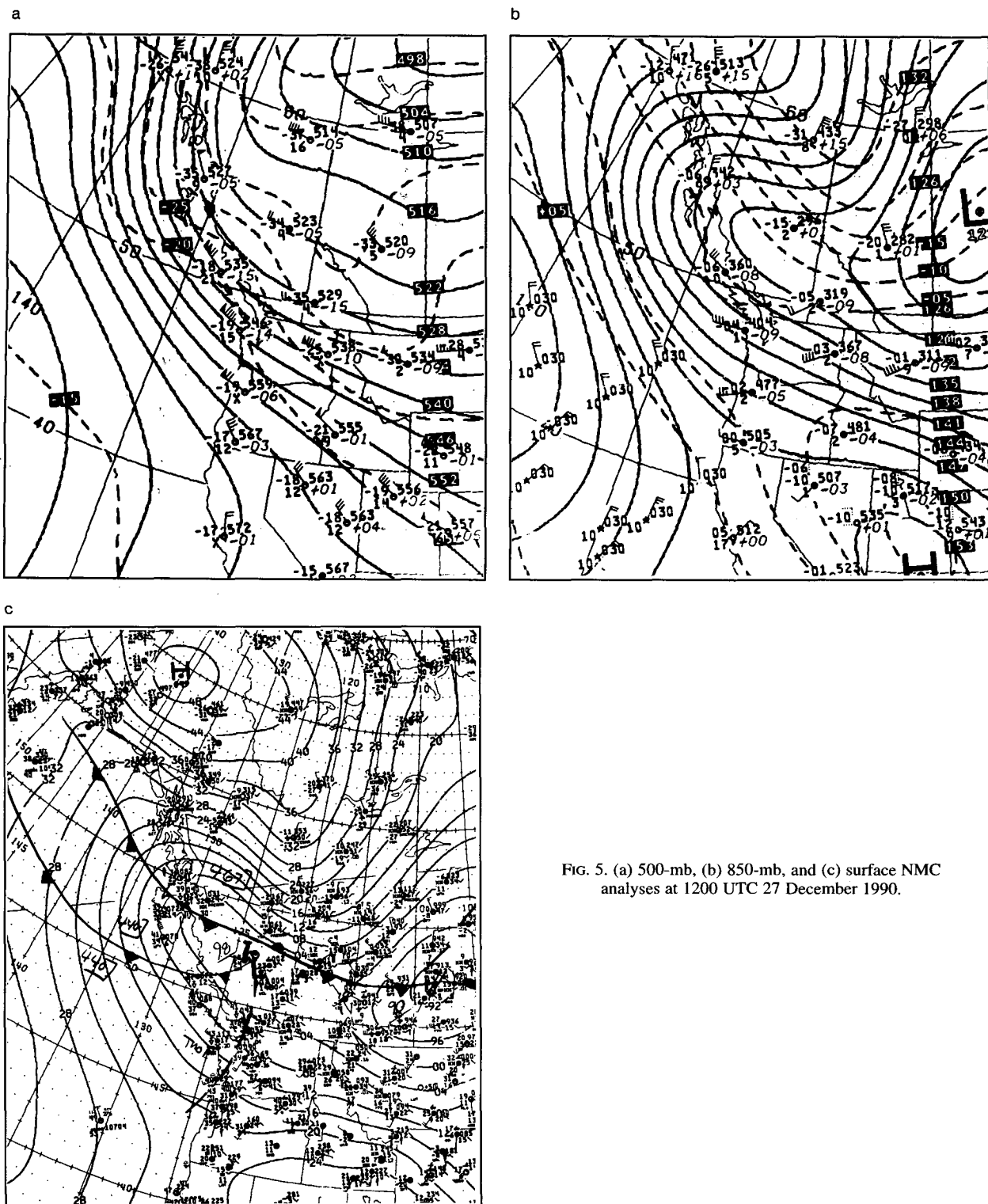


FIG. 5. (a) 500-mb, (b) 850-mb, and (c) surface NMC analyses at 1200 UTC 27 December 1990.

over northeast Washington. The zone of large horizontal temperature gradient was now over southern British Columbia, and generally northwesterly flow was evident over western Washington. A synoptic-scale sur-

face analysis at this time (Fig. 6c) reveals that the pressure trough was near the international border and extended offshore along the British Columbia coast. A mesoscale analysis (Fig. 6d) indicates that arctic air







pressure gradient over southern British Columbia and northern Washington (Fig. 9c). Sea level pressure had risen rapidly over southern British Columbia due to the southward retreat of the upper-level synoptic trough and the influx of cold air at low levels behind it. The regional mesoscale analysis at this time (Fig. 9d) shows the continued existence of a trough extending from the central Cascades into northwest Washington, the large pressure difference along the Fraser Gap (10.4 mb between Hope and Bellingham) and over northwest Washington, mesoscale ridging along the eastern slope of Vancouver Island, and the pressure ridge due to cold-air damming over eastern Washington. By this time, northerly flow had pushed southward into southern Puget Sound.

At 1800 UTC, both the regional mesoscale analysis (Fig. 10) and observations at BLI (Table 1) show that although winds had begun to weaken slightly around Bellingham, the northerly winds over Puget Sound had strengthened considerably. The synoptic trough had shifted south of Washington and a tongue of lower pressure extended northward into northwest Washington. Strong northerlies and mesoscale damming had moved southward along the eastern slopes of the Cascades. Temperatures had dropped into the teens (°F) over much of northwest Washington, while eastern Washington had cooled into the single digits (°F).

By 0000 UTC 29 December the 500-mb short-wave trough had moved southeast of Washington (not shown). At 850 mb, the low center had moved southeastward into Utah, coastal troughing had weakened, and temperatures over Washington had dropped considerably compared to 12 h earlier (Fig. 11). The surface mesoscale analysis at this time (not shown) is quite similar to the 1800 UTC chart (Fig. 10), with the primary exception of weaker winds. Gradual weaken-

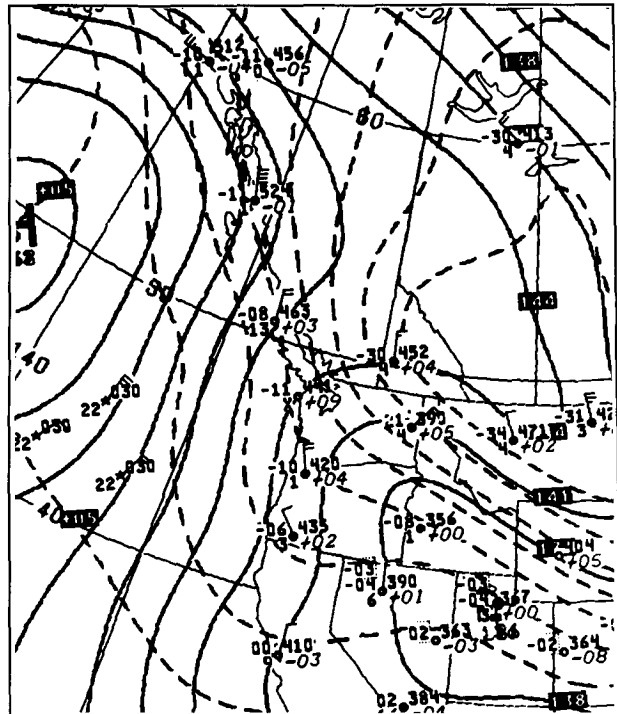


FIG. 11. The 850-mb NMC analysis at 0000 29 December 1990.

ing of the winds and associated pressure gradients continued over the next 12 h, as the coldest air spread over the region.

*b. Vertical structure*

Figure 12 presents soundings at Vernon, British Columbia (YXO), and Quillayute, Washington (UIL), the two nearest radiosonde locations to the area of interest (see Fig. 1 for locations). Soundings at Vernon (555 m ASL), located on the eastern side of the Coast Range, provide insight into the movement and depth of arctic air within the southern interior of British Columbia, while vertical profiles at Quillayute (62 m ASL) indicate the structure of the arctic air mass along the northern Washington coast. At 0000 UTC 28 December 1990, the Vernon sounding (Fig. 12a) shows a shallow (~50 mb) layer of cold air immediately above the surface that is surmounted by an inversion with a base at approximately 900 mb. Winds near the surface are light, while above 900 mb the winds veer into the northwest and strengthen. Twelve hours later (1200 UTC 28 December), proximate in time to the highest wind speeds at Bellingham, substantial cooling has occurred in the Vernon sounding below 600 mb and a near-adiabatic layer extends from the surface to about 820 mb. The near-surface winds have greatly strengthened and are from the northwest, gradually veering from the surface to 700 mb and then abruptly backing to westerly at 650 mb.

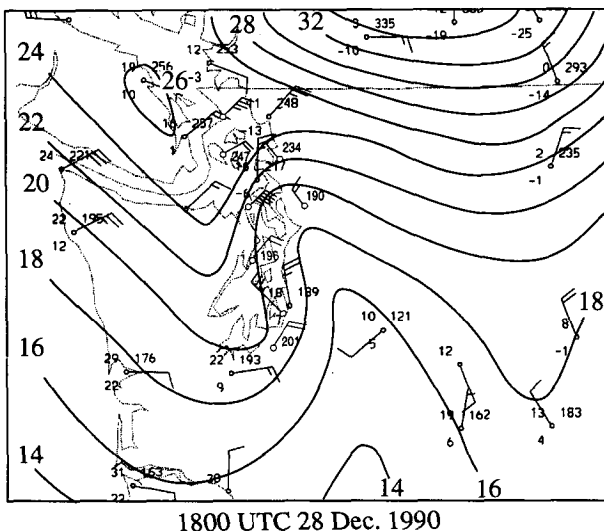


FIG. 10. Mesoscale surface analysis at 1800 UTC 28 December.

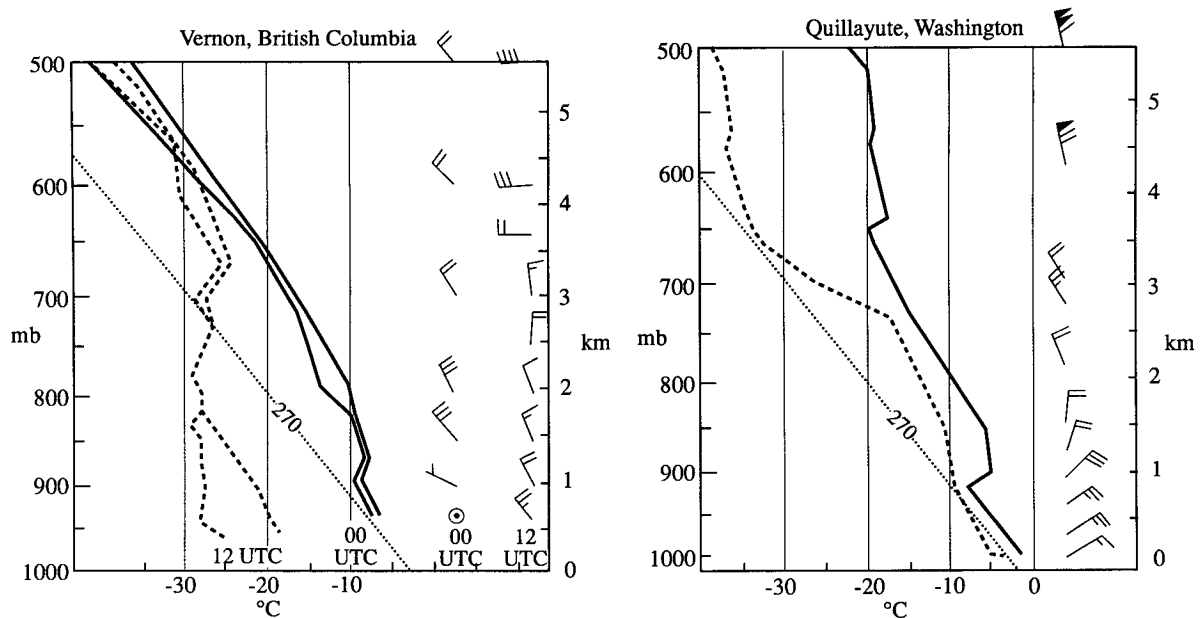


FIG. 12. (a) Vertical soundings of temperature and dewpoint at Vernon, British Columbia, at 0000 and 1200 UTC 28 December, and (b) at Quillayute, Washington, at 1200 UTC 28 December 1990.

Prior to the windstorm (0000 UTC 28 December), there was no hint of arctic air in the Quillayute sounding, with approximately a saturated-adiabatic lapse rate and relatively uniform northwesterly winds from the surface to 600 mb (not shown). By 1200 UTC 28 December (Fig. 12b), the influx of cold arctic air at low levels resulted in a well-mixed, dry-adiabatic layer from the surface to approximately 920 mb ( $\sim 900$  m); this layer was capped by an inversion and isothermal layer that extended to 850 mb. At this time, the low-level winds were northeasterly from the surface up to approximately 850 mb, with backing into the northwest above.

To understand the 28 December 1990 windstorm, it would be useful to examine a sounding at the terminus of the Fraser Gap near Bellingham, Washington. Although no soundings are taken at that location, it is possible, using the method discussed in Reed (1981), to estimate the vertical temperature profile. First, the surface temperature and pressure observations at BLI for 1200 UTC 28 December (near the time of the maximum wind speed) were acquired, and the heights and temperatures at 850 and 700 mb above that location were interpolated subjectively from manual analyses at these levels. From these height values the mean virtual temperature in the 1000–850-mb and 1000–700-mb layers were calculated using the hypsometric equation. (The 1000-mb height was calculated using the sea level pressure and a lapse rate of 1 mb per 8 m.) Because of the cold temperatures at this time, temperature and virtual temperature for these layers differ by less than 0.5°C. To diagnose the vertical structure over Belling-

ham, 12-h backward isentropic trajectories ending at 850 and 700 mb above this location at 1200 UTC 28 December were calculated graphically (Saucier 1972, 312–313) to find the origin of the air in the lower troposphere; this exercise indicated that the trajectories ending over Bellingham in the layer from 700 to 850 mb began in the vicinity of the radiosonde site at Prince George, located in central British Columbia, at 0000 UTC 28 December 1990. The Prince George sounding at this time (Fig. 13) shows a deep adiabatic mixed layer to approximately 780 mb, surmounted by an inversion from 2 to 4 km. Such midtropospheric inversions are associated with most arctic intrusions in this region, with the base of the inversions generally located at the mean crest level of the regional orography (typically about 2500 m). The mechanisms producing such inversions are discussed in Reed (1981) and Mass and Albright (1985).

The Bellingham sounding at 1200 UTC 28 December was then constructed by noting that near the surface the sounding should be approximately dry adiabatic due to mixing accompanying the strong, gusty winds at low levels. Then the 0000 UTC 28 December Prince George sounding was lowered approximately dry adiabatically into the surface-based mixed layer until the temperatures at 850 and 700 mb closely matched the horizontally interpolated values over Bellingham and the 1000–700-mb and 1000–850-mb layer-mean virtual temperatures approximated the previously diagnosed values at that location. To produce the optimal match of the various temperatures and thicknesses, the Prince George

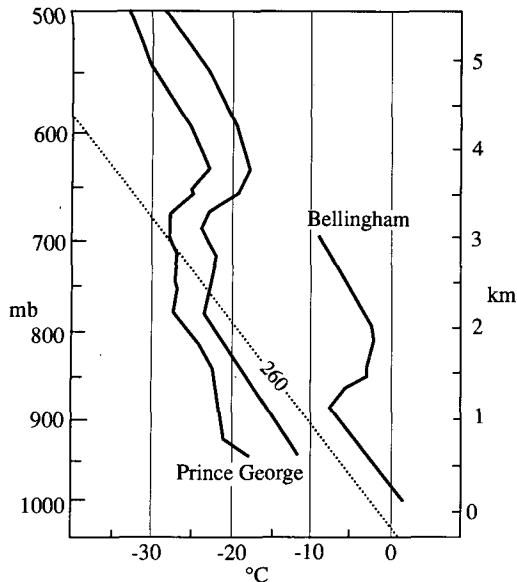


FIG. 13. Vertical sounding at Prince George, British Columbia, at 0000 UTC 28 December 1990 and a constructed temperature sounding at Bellingham, Washington, for 1200 UTC 28 December 1990.

sounding was lowered more at lower elevations, consistent with the isentropic pattern found in previous studies (e.g., Reed 1981). The resulting Bellingham sounding, also shown in Fig. 13, has a surface-based mixed-layer depth of approximately 1100 m, quite close to the depths observed in Howe Sound (the next gap to the north) during another arctic air outbreak (Jackson and Steyn 1994). The above mixed-layer thickness is also consistent with observations made by Overland and Walter (1981) (using dropsondes from a NOAA P3 aircraft) over the eastern Strait of Juan de Fuca during another arctic air intrusion. In the synthetic Bellingham sounding the cold mixed layer is surmounted by an inversion that extends to about 1.8 km, with a nearly saturated-adiabatic lapse rate above.

The 1100-m mixed-layer depth at Bellingham is also consistent with the height calculated using a completely different approach, that is, by applying the hydrostatic equation to determine how deep of a layer had to be cooled (by the amount observed at the surface at Bellingham) to produce the observed pressure rise at the surface (for the period 0000–1200 UTC 28 December). The contribution to the surface pressure tendency by the observed changes in 850-mb height over Bellingham (derived by subjectively interpolating manual analyses at this level) was considered in this analysis. The resulting mixed-layer depth over Bellingham at 1200 UTC 28 December was 1033 m, within 10% of the 1100 m calculated using the other method. In the subsequent analyses, a mixed-layer height of 1050 m at Bellingham is used.

#### 4. Analysis and discussion

This section attempts to explain the low-level wind distribution observed during the 28 December 1990 event, and particularly the origin of the strong winds that struck the islands downstream of the Fraser Gap. It will be shown that the complex wind field observed during this windstorm resulted from the interaction among several effects, including down-gradient flow within the gap region, troughing in the lee of the Cascade Mountains, and differential drag over land and water. The potential of smaller-scale effects such as local blocking and channeling by the terrain, and boundary layer vortical motions are also examined.

The large sea level pressure gradient over portions of northwest Washington near the time of strongest winds (0900 UTC 28 December, Fig. 8) is consistent with a geostrophic wind speed of approximately  $150 \text{ m s}^{-1}$  and a gradient wind of  $48 \text{ m s}^{-1}$ , the latter being slightly less than the maximum surface wind observed over the region. However, considering the rapid acceleration of air parcels near the surface as they quickly traversed the Fraser Gap and then proceeded over northwest Washington (a 1.5-h trip from Hope to Bellingham at  $20 \text{ m s}^{-1}$ ) and the small spatial scale of the mesoscale troughing and ridging over northwest Washington, there is little possibility that either geostrophic or gradient wind balance could have been established. Thus, a different explanation of the intense winds is required.

##### a. Flow acceleration within the Fraser River gap

Surface wind and damage reports (e.g., Figs. 9d and 10) suggest that the low-level high-speed air that struck northwest Washington had exited the Fraser Gap. In this section, the origin of this air and its acceleration within the gap will be examined.

As shown in Fig. 1, the Fraser Gap narrows to the east. Since the large volume of air exiting the western terminus of this gap could not have come from the narrow river valleys that meet in the vicinity of Hope, British Columbia, a considerable amount of air must have passed over and down the mountain slopes surrounding the eastern end of the gap. This hypothesis is also supported by the fact that the potential temperature at Hope near the height of the windstorm (259.3 K at 1200 UTC 28 December) was nearly identical to the potential temperature measured simultaneously within the well-mixed deep arctic air mass at Vernon, on the other side of the Cascade Mountains (cf., Fig. 12a).

After descending into the eastern section of the Fraser Gap, the air was accelerated southwestward by the large synoptic-scale pressure gradient overlying this region. The along-gap pressure gradient was also strengthened by the decreasing height of the cold, arctic

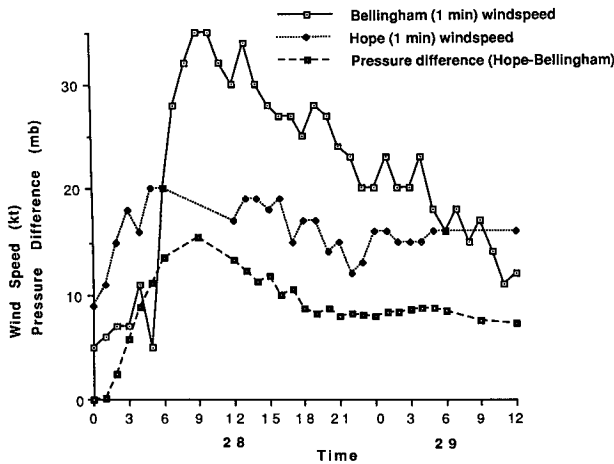


FIG. 14. One-minute average wind speed at Bellingham, Washington, and Hope, British Columbia, and the sea level pressure difference between the two stations during the 28 December 1990 windstorm.

air as it accelerated eastward down the gap. Figure 14 presents the 1-min average winds observed at Bellingham, Washington (BLI), and Hope, British Columbia (YHE), at the western and eastern termini of the Fraser Gap, respectively. In addition, the sea level pressure difference between the two stations is shown. [BLI and YHE are both located near sea level at elevations of 48 and 38 m ASL, respectively.] At Hope, 1-min winds increased rapidly from approximately 5 to 10 m s<sup>-1</sup> (10 to 20 kt) between 0000 and 0600 UTC 28 December following passage of the arctic front. Nearly simultaneously, the pressure difference between BLI and YHE increased from near 0 to about 15 mb, primarily because of the sharply higher pressures at the latter station after frontal passage. As discussed in Overland and Walter (1981) and Overland (1984), such a large along-gap pressure gradient should result in strong ageostrophic acceleration down the gap. Such acceleration is indicated by the mesoscale surface charts and the relative wind speeds at Hope and Bellingham (Fig. 14). Specifically, the 1-min wind speed at Hope, at the eastern end of the gap, increased by approximately 5 m s<sup>-1</sup> (10 kt), while at Bellingham Airport (BLI), at the western exit, the 1-min average wind jumped by 15 m s<sup>-1</sup> (30 kt) between 0000 and 0600 UTC 28 December. Even stronger winds were observed a few kilometers north of BLI within the center of the current. The few-hour delay between the increase in the YHE-BLI pressure difference and the rapid increase in wind speed at Bellingham is not surprising since the pressure difference is for a region upwind of the wind observation.

As noted by Reed (1981), frictionless, steady-state flow within a constant-elevation channel can be described by an integrated form of the Bernoulli equation that expresses a balance between the along-gap pres-

sure gradient force and inertia (or equivalently, advection):

$$\frac{u_2^2}{2} = \frac{u_1^2}{2} - \frac{\Delta p}{\rho}, \quad (1)$$

where  $u_1$  ( $u_2$ ) is the entrance (exit) velocity along the channel,  $\Delta p$  is the pressure difference along the channel ( $p_2 - p_1$ ), and  $\rho$  is the density. In the present case, the entrance and exit locations are approximated by YHE and BLI, respectively. Equation (1) is then applied to the period of near maximum winds (about 0900 UTC 28 December), during which the winds and pressure gradients were approximately steady. Referring to Fig. 14, at this time the interpolated 1-min winds at Hope were approximately 10 m s<sup>-1</sup> and the pressure difference between the two sites was 14 mb. Substituting these values into (1), using a density of 1.35 g kg<sup>-1</sup> (based on the average density at the two sites), gives a value of 46 m s<sup>-1</sup>, a value far in excess of the observed 1-min average wind speed at BLI of 17.5 m s<sup>-1</sup> (35 kt) or the estimated 1-min wind speed (~30–35 m s<sup>-1</sup>) in the core of the current 5–10 km to the north. The 46 m s<sup>-1</sup> wind speed estimated by (1) does, however, closely approximate the maximum gust experienced within the center of the current.

Overland (1984) and Lackman and Overland (1989) have shown through scale analysis that friction is also important within gaps; thus, one might expect that a three-way balance between inertia, friction, and the imposed pressure gradient should produce a superior relationship than (1) for explaining down-gap acceleration. As derived in the appendix, such a relationship has the form

$$u^2(x) = \left[ u^2(0) - \frac{P_x}{K} \right] e^{-2Kx} + \frac{P_x}{K}, \quad (2)$$

where  $u(0)$  is the initial wind speed,  $u(x)$  is the wind speed some distance  $x$  from the starting point along the gap,  $P_x$  is the along-gap pressure gradient force, and  $K$  (described in the appendix) is a friction coefficient that is a function of surface roughness, stability, and boundary layer depth. Mesoscale model simulations by Jackson and Steyn (1994) of the flow down Howe Sound, the next major gap to the north, and simple continuity arguments suggest that the depth of the arctic air should decrease as it accelerates down the Fraser Gap. Averaging the previously estimated arctic air depth at Bellingham (1050 m) and the thickness of the arctic air mass (1472 m) at Vernon, just upstream of the gap, produces a mean depth over the gap of 1261 m. Using this boundary layer depth and a drag coefficient  $C_D$  suitable for a land area of moderate roughness ( $7.5 \times 10^{-3}$ , taken from Arya 1988, p. 153) results in a  $K$  of  $1.7 \times 10^{-5} \text{ m}^{-1}$ . Using a distance of 110 km and a pressure difference of 14 mb between Hope and Bellingham, a density of 1.35 kg m<sup>-3</sup>, a  $P_x$  of  $9.4 \times 10^{-3} \text{ N kg}^{-1} \text{ m}^{-1}$ , the  $K$  value noted above, and an initial

wind speed of  $10 \text{ m s}^{-1}$  at Hope, results in a predicted 1-min wind speed at BLI [using Eq. (2)] of  $23.3 \text{ m s}^{-1}$  (46.6 kt). This speed is far less than the  $46 \text{ m s}^{-1}$  calculated using (1), illustrating the importance of surface drag.

At BLI, the maximum gust (over a 10-min period prior to the observation time) and the peak instantaneous wind (over the preceding 1 h) during the time of strongest winds (at about 0900 UTC 28 December) were  $27.5 \text{ m s}^{-1}$ . Thus, there was a ratio of 1.57 between the maximum gust and the 1-min average wind speed ( $17.5 \text{ m s}^{-1}$ ) at this time. Similar ratios have been observed over land stations in western Washington during other periods of high winds. Applying this factor to the calculated 1-min wind speed ( $23.3 \text{ m s}^{-1}$ ), suggests a maximum gust of  $36.6 \text{ m s}^{-1}$  (73.2 kt, 84.2 mph). Although the estimated 1-min wind speed and gust are approximately 33% larger than observed at BLI, they are consistent with observations and damage in the core of the current, a few kilometers to the north.

#### b. Flow acceleration and channeling downstream of the gap exit

As strong northeasterly flow moved out of the Fraser Gap it soon passed over water (see Fig. 1). As described in Hsu (1988), this transition results in acceleration because of reduced surface drag over water. Furthermore, because the arctic air was considerably cooler than the relatively warm water of the Puget Sound/Strait of Georgia ( $-9^{\circ}\text{C}$  vs  $+7^{\circ}\text{C}$ ), vertical stability is reduced, resulting in greater mixing of higher momentum air from aloft. Offshore acceleration for such situations is usually very rapid, generally occurring within a few kilometers of shore (Roeloffzen et al. 1986; Hsu 1988).

The ratio of water to land surface wind speeds can be calculated using the relationship found in Liu et al. (1984):

$$\frac{U_{\text{water}}}{U_{\text{land}}} = \left( 1.2 + \frac{1.85}{U_{\text{land}}} \right) \phi(\Delta T), \quad (3)$$

$$\phi(\Delta T) = 1 - \frac{\Delta T}{|\Delta T|} \left( \frac{|\Delta T|}{1920} \right)^{1/3}, \quad (4)$$

where  $\Delta T$  is the air–water temperature difference ( $^{\circ}\text{C}$ ). Applying this relationship for a  $\Delta T$  of  $-16^{\circ}\text{C}$  results in a ratio of 1.54 between the winds over the water and land. Using this factor with the estimated 1-min wind speed in the core of the current over land calculated using (2) of  $23.3 \text{ m s}^{-1}$ , results in an estimated 1-min wind speed over the water of  $35.9 \text{ m s}^{-1}$  (71.8 kt) within a few kilometers offshore. Over water the ratio of gusts to 1-min average winds is less than over land (because of the lesser surface roughness). Observations of such ratios at bridge locations in western Washington suggest gust to 1-min wind ratios of

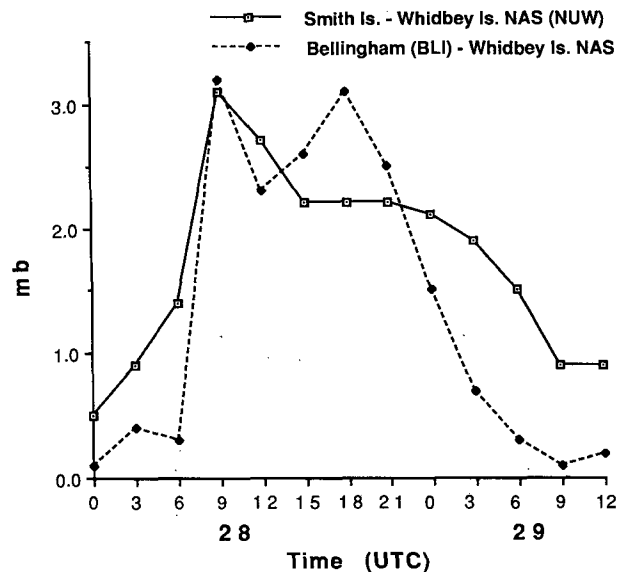


FIG. 15. Pressure differences (mb) between Whidbey Island Naval Air Station and both Bellingham Airport and Smith Island.

1.25–1.30 (R. J. Reed 1992, personal communication). Using a ratio of 1.27, results in an estimated gust of  $45.6 \text{ m s}^{-1}$  (91.2 kt, 104.9 mph) over the water, within  $1\text{--}2 \text{ m s}^{-1}$  of the maximum gusts observed on the windward (northeast) shore of Lummi Island.

Because of the strong pressure gradient over northwest Washington during the height ( $\sim 1200$  UTC 28 December) of the windstorm, there was the potential for additional downgradient acceleration downstream of the Fraser Gap. Figure 15, which shows the sea level pressure difference between Bellingham (BLI) and NUW, indicates that this pressure difference increased rapidly from near 0 to approximately 3 mb between 0600 and 0900 UTC 28 December. As shown in the surface mesoscale analyses at 0900 and 1200 UTC 28 December (Figs. 8 and 9d), troughing in the lee of the Cascade Range and (to a lesser extent) ridging on the windward (eastern) side of Vancouver Island contributed to the development of this gradient. A measure of the intensity of the lee troughing is the pressure difference between NUW and Smith Island, 15 km to the west/southwest; as shown in Fig. 15, this pressure difference increased rapidly between 0300 and 0900 UTC 28 December.

To calculate the expected acceleration between Bellingham and Guemes Island due to the pressure gradient over the lowlands of northwest Washington, the pressure difference between BLI and NUW was used (the mesoscale analyses in Figs. 8 and 9d suggest that the pressure difference between Bellingham and Guemes Island should be similar to the BLI – NUW value, that is, 3 mb). Using an initial 1-min wind speed over water of  $35.9 \text{ m s}^{-1}$ , a distance of 30 km, a mixed-

layer depth of 771 m,<sup>7</sup> and a drag coefficient of  $1.5 \times 10^{-3}$  in Eq. (2) results in a 1-min speed of  $36.2 \text{ m s}^{-1}$  at Guemes, a minor additional acceleration of only  $0.3 \text{ m s}^{-1}$ . Thus, the gradient downwind of the gap served only to prevent deceleration due to surface drag. Using the over-water gust to 1-min average wind speed ratio applied above (1.27) results in an estimated gust in the vicinity of Guemes Island of  $46 \text{ m s}^{-1}$  (92 kt, 106 mph), a speed consistent with the damage observed on the island and the anemometer reading at Anacortes.

Several individuals on Guemes Island and other locations within the strong northeasterly wind current noted that there was considerable periodic variability in wind strength. For example, one observer on Guemes Island (Joost Businger 1994, private communication) noted that winds would build and then decrease over a period of approximately 10 min. A possible explanation of this variability is the existence of coherent eddy structures within the boundary layer. For example, the planetary boundary layer often is organized into roll vortices (Etling and Brown 1993); associated with such rolls there are regions of enhanced upward and downward motion, the former (latter) being associated with decreased (increased) low-level wind speeds (downward motion brings down higher momentum from aloft).<sup>8</sup> Another type of coherent structure in the boundary layer is the "hairpin" or "horseshoe vortex," which is driven by the shear in the viscous sublayer (Gerz et al. 1994; Tritton 1988, 344–350). The movement and evolution of a field of such coherent structures might explain some of the temporal variability of the strong winds noted above. Smaller-scale mobile vortices, possibly forced by the interaction of the strong flow with underlying island topography, could have occurred during this case. Such vortices have been observed during Boulder downslope windstorms and apparently contribute to inhomogeneities in damage during such events (Zipser and Bedard 1982).

<sup>7</sup> To calculate the boundary layer depth over water, we began with an initial boundary layer depth of 1050 m over land (see section 3b) and a simple continuity relationship relevant to the transition from land to water,  $U_L H_L = U_W H_W$ , where  $U_L$  and  $U_W$  are the mean 1-min mixed-layer winds and  $H_L$  and  $H_W$  are the mixed-layer heights over land and water, respectively. These winds were calculated by averaging the surface 1-min average wind and the maximum gust, assuming that the gust represents the mean, 1-min wind near the top of the mixed layer. With such an approach the  $U_L$  and  $U_W$  are 29.9 and  $40.7 \text{ m s}^{-1}$ , respectively, resulting in an overwater boundary layer depth of 771 m. Of course, this calculation does not include the effects of lateral spreading and vertical entrainment, but simply serves as a rough estimate for showing the lack of importance of pressure gradient acceleration downwind of the gap.

<sup>8</sup> The horizontal scale of individual rolls is approximately the height of the mixed layer and thus regions of descending motion (and strong winds) would be spaced at horizontal distances of approximately twice the height of the boundary layer.

The possibility that the strong winds over northwest Washington resulted from a downslope windstorm mechanism as observed in Boulder, Colorado (Brinkmann 1974; Zipser and Bedard 1982; Durran 1986), was considered and dismissed. As with the Boulder windstorms there was an inversion at crest level (cf., the Vernon sounding in Fig. 12) and at least some cross-mountain flow (as suggested by the troughing in the lee of the Cascades, see Fig. 8). But unlike downslope windstorm events, the strongest winds were not observed in the immediate lee of major topographic barriers and the strong flow was organized in an elongated mesoscale current that was clearly associated with the gap. Furthermore, during the 28 December 1990 event, cross-mountain flow near crest level ( $10\text{--}20 \text{ m s}^{-1}$ ) was considerably weaker than the flow described in the windstorm literature for Boulder (Brinkmann 1974).

As noted in section 2, the strong winds were isolated within a relatively narrow current, which maintained its integrity and sharp boundaries at least 50–100 km beyond the terminus of the Fraser Gap. As noted in Overland and Walter (1981), such jet maintenance has been observed for other northeasterly gap flow events over northwest Washington and for outflow events near Big Delta, Alaska. Mass and Albright (1985) showed that the outflow through the higher Stampede Gap of the central Washington Cascades was organized into a sharply defined current over the Puget Sound region and that this current maintained its integrity over 100 km offshore of the Washington coast. A recent simulation of the drainage flows over northwest Washington using a shallow-water model (Simon Ward 1994, private communication) produced a current exiting the Fraser Gap with many of the characteristics noted above (e.g., sharply defined boundaries, maintenance well beyond the gap). Explaining the sharp boundaries and longevity of such jets outside of their generation region (i.e., the gaps in the terrain) is a significant theoretical question that remains unanswered.

Another interesting aspect of this event was the rapid decrease in the maximum winds south of Lopez and Fidalgo Islands. For example, NUW, located only 20 km south of Anacortes (on northern Fidalgo Island), had a maximum gust of only  $25.5 \text{ m s}^{-1}$  (51 kt), while at Smith Island, a similar distance to the south-southwest of Anacortes and surrounded by water, the winds reached only  $22 \text{ m s}^{-1}$  (44 kt). Perhaps a hydraulic jump occurred as the northeasterly flow fanned out into Puget Sound and the Strait of Juan de Fuca. In addition, as shown by the mesoscale analyses (e.g., Figs. 8 and 9b), the pressure gradient weakened considerably to the south and west.

## 5. Conclusions and summary

During 28 December 1990, northeasterly flow exceeding  $45 \text{ m s}^{-1}$  struck sections of northwest Wash-

ington, resulting in extensive property damage, injuries, and loss of life, as well as widespread power outages. In the lower troposphere, cold arctic air entered the interior of British Columbia, while aloft a strong short-wave trough approached the Pacific Northwest; the cold air progressively increased in depth and, nearly coincident with short-wave passage aloft, descended into the eastern terminus of a mesoscale gap in the Coast mountains (the Fraser Gap). The cold air then accelerated (at nearly constant elevation) under the influence of a large horizontal pressure gradient toward the western exit of the gap near Bellingham, Washington. This gap acceleration was quantitatively explained by a three-way balance among the pressure gradient force, friction, and inertia.

The northeasterly flow, approximately 1 km in depth, was limited to a well-defined mesoscale current that maintained its integrity well beyond the terminus of the gap. Above the low-level gap current, there was northeasterly flow that originated in the middle troposphere to the north over central British Columbia and then descended the high terrain north of the gap. This upper northeasterly airstream was potentially too warm to reach the surface and contributed to the inversion that capped the cold gap flow. Upon reaching water, the low-level gap flow accelerated by approximately 50% and the height of the capping inversion dropped. Troughing in the lee of the Cascade Mountains enhanced the horizontal pressure gradient over northwest Washington; the corresponding pressure gradient force approximately balanced frictional drag, resulting in only minimal, acceleration. Further south the flow decelerated as the current spread out horizontally.

*Acknowledgments.* The authors would like to acknowledge the valuable comments and suggestions of Nick Bond, Robert Brown, Brad Colman, Gad Levy, Yuh-Lang Lin, Richard Reed, Jim Steenburgh, and Douw Steyn, the assistance of Ernie Recker and Joe Tenerelli in acquiring observational data, Brian Colle in producing the topographic map, and David Dempsey for deriving the frictional gap wind formula. This research was funded in part from two subawards (NA90AA-H-AC781, NA37W00018-01) under a cooperative agreement between the National Oceanic and Atmospheric Administration and the COMET Program in the University Corporation for Atmospheric Research (UCAR). The views expressed herein are those of the authors and do not necessarily reflect the views of NOAA, its subagencies, or UCAR. Support was also provided by the National Science Foundation (ATM-9121126, ATM-8912472, and ATM-9111011).

#### APPENDIX

##### Analytical Solution for a One-Dimensional Balance Between the Pressure Gradient Force, Advection, and Parameterized Friction

Under steady, one-dimensional conditions with an imposed along-gap pressure gradient (independent of

distance down the gap,  $x$ ), the force balance within a gap can be written (Overland 1984):

$$u \frac{\partial u}{\partial x} = F + P_x, \quad (\text{A1})$$

where  $F$  represents the frictional force,  $P_x$  is the pressure gradient force ( $-\rho^{-1} \partial p / \partial x$ ), and  $u$  is the wind speed in the along-gap direction  $x$  ( $x$  increases down the gap from high to low pressure). The frictional force at the surface can be represented (assuming wind is only in the  $x$  direction) by the convergence of vertical momentum flux with height

$$F = - \frac{\partial \overline{u'w'}}{\partial z}. \quad (\text{A2})$$

Next, it is assumed that the momentum flux at the surface can be calculated using the bulk aerodynamic formula

$$\overline{u'w'} = -C_D U^2, \quad (\text{A3})$$

where  $C_D$  is the appropriate drag coefficient, and that the momentum flux falls off to zero at a height of  $H/2.8$ , where  $H$  is the height of the well-mixed boundary layer. The factor 2.8 was suggested by Deardorff (1972) to account for the fact that for neutral and stable boundary layers the stress vanishes considerably lower than the top of the thermal boundary layer. With the above assumptions, the friction force at the surface can be parameterized by

$$F = -Ku^2, \quad (\text{A4})$$

where  $K$  is equal to  $C_D(2.8/H)$ .

Substituting (A4) into (A1) results in the expression

$$\frac{\partial u^2}{\partial x} = -2Ku^2 + 2P_x. \quad (\text{A5})$$

This ordinary, first-order, differential equation with  $u^2$  as the dependent variable can be solved by first multiplying (A5) by  $2^{2Kx}$  and then integrating from 0 to  $x$ . The result is

$$u^2(x) = \left[ u^2(0) - \frac{P_x}{K} \right] e^{-2Kx} + \frac{P_x}{K}. \quad (\text{A6})$$

An interesting consequence of (A6) is that for sufficiently large  $x$ , the initial wind speed is relatively unimportant and that the flow is antitriptic [i.e., there is a balance between the pressure gradient force and friction, with advection (inertia) being negligible].

A factor neglected in the derivation of (A6) that would have produced additional wind reduction is entrainment at the top of the boundary layer. Lackman and Overland (1989), in a study of gap flow through the Shelikof Strait off the southern coast of Alaska, found that the drag from such vertical entrainment was approximately as large as surface friction. However, there are several reasons why such entrainment would

be less important (compared to surface friction) for the 28 December event. First, the Lackman and Overland case was over a relatively smooth water surface, in contrast to the continental location (with numerous roughness elements such as hills and trees) of the December 1990 case. Second, as shown in Figs. 12 and 13, a considerably stronger stable layer capped the channeled flow through the Fraser Gap than for the corresponding current through the Shelikof Strait; such stability would tend to reduce turbulence and vertical entrainment. Finally, since the flow at 850 mb over the gap appears to be from the northeast (e.g., Fig. 9b), there is less shear between the top of the gap flow and the overlying air mass for the December event, resulting in weaker turbulence and less vertical momentum transport.

## REFERENCES

- Arya, S. P., 1988: *Introduction to Micrometeorology*. Academic Press, 307 pp.
- Bedard, A. J., Jr., 1990: A review of the evidence for strong, small-scale vortical flows during downslope windstorms. *J. Wind Eng. Ind. Aero.*, **36**, 97–106.
- Brinkmann, W. A. R., 1974: Strong downslope winds at Boulder, Colorado. *Mon. Wea. Rev.*, **102**, 592–602.
- Deardorff, J. W., 1972: Parameterization of the planetary boundary layer for use in general circulation models. *Mon. Wea. Rev.*, **113**, 89–98.
- Dickey, W. W., and R. N. Wing, 1963: The unusual: Arctic air into the Pacific Northwest. *Weatherwise*, **23**, 259–263.
- Durran, D., 1986: Another look at downslope windstorms. Part I: The development of analogs to supercritical flow in an infinitely deep, continuously stratified fluid. *J. Atmos. Sci.*, **43**, 2527–2543.
- Etling, D., and R. A. Brown, 1993: Roll vortices in the planetary boundary layer: A review. *Bound.-Layer Meteor.*, **65**, 215–248.
- Ferber, G. K., C. F. Mass, G. M. Lackmann, and M. W. Patnoe, 1993: Snowstorms over the Puget Sound lowlands. *Wea. Forecasting*, **8**, 481–504.
- Gerz, T., J. Hoel, and L. Mahrt, 1994: Vortex structures and microfronts. *Phys. Fluids*, **6**(3), 1242–1251.
- Hsu, S. A., 1988: *Coastal Meteorology*. Academic Press, 260 pp.
- Jackson, P. L., and D. G. Steyn, 1994: Gap winds in a fjord. Part I: Observations and numerical simulation. *Mon. Wea. Rev.*, **122**, 2645–2665.
- Liu, P. C., Schwab, D. J., and Bennett, J. R., 1984: Comparison of a two-dimensional wave prediction model with synoptic measurements in Lake Michigan. *J. Phys. Oceanogr.*, **14**, 1514–1518.
- Lackman, G. M., and J. E. Overland, 1989: Atmospheric structure and momentum balance during a gap-wind event in Shelikof Strait, Alaska. *Mon. Wea. Rev.*, **117**, 1817–1833.
- Lilly, K. E., 1983: Marine weather of western Washington. Starpath School of Navigation, Seattle, Washington, 146 pp.
- Mass, C. F., 1981: Topographically-forced convergence in western Washington State. *Mon. Wea. Rev.*, **109**, 1335–1347.
- , and M. D. Albright, 1985: A severe windstorm in the lee of the Cascade Mountains of Washington State. *Mon. Wea. Rev.*, **113**, 1261–1281.
- Overland, J. E., 1984: Scale analysis of marine winds in straits and along mountainous coasts. *Mon. Wea. Rev.*, **112**, 2532–2536.
- , and B. A. Walter, 1981: Gap winds in the Strait of Juan de Fuca. *Mon. Wea. Rev.*, **109**, 2221–2233.
- Reed, R. J., 1981: A case study of a bora-like windstorm in western Washington. *Mon. Wea. Rev.*, **109**, 2383–2393.
- Roeloffzen, J. C., W. D. Van Den Berg, and J. Oerlemans, 1986: Frictional convergence at coastlines. *Tellus*, **38A**, 397–411.
- Saucier, W. J., 1972: *Principles of Meteorological Analysis*. The University of Chicago Press, 438 pp.
- Tritton, D. J., 1988: *Physical Fluid Dynamics*. Oxford University Press, 519 pp.
- Zipsper, E. J., and A. J. Bedard, 1982: Front Range windstorms revisited. *Weatherwise*, **35**, 82–85.